

## Microstructural Analysis of a Cubic Bicontinuous Morphology in a Neat SIS Triblock Copolymer

Jonathan H. Laurer,<sup>†</sup> Damian A. Hajduk,<sup>‡,§</sup>  
Jennifer C. Fung,<sup>||</sup> John W. Sedat,<sup>⊥</sup>  
Steven D. Smith,<sup>○</sup> Sol M. Gruner,<sup>‡</sup>  
David A. Agard,<sup>⊥,¶</sup> and Richard J. Spontak<sup>\*†</sup>

Department of Materials Science & Engineering, North Carolina State University, Raleigh, North Carolina 27695, Department of Physics, Princeton University, Princeton, New Jersey 08544, Graduate Group in Biophysics, University of California, San Francisco, California 94143, Department of Biochemistry and Biophysics, University of California, San Francisco, California 94143, Corporate Research Division, The Procter & Gamble Company, Cincinnati, Ohio 45239, and Howard Hughes Medical Institute, University of California, San Francisco, California 94143

Received April 1, 1997

Morphological investigations of neat block copolymers, as well as copolymer/copolymer and copolymer/homopolymer blends, have revealed the existence of fascinating complex morphologies, such as the gyroid (G),<sup>1–6</sup> perforated lamellar (PL)<sup>1,2,7–9</sup> or lamellar catenoid (LC),<sup>10–12</sup> and sponge (L<sub>3</sub>)<sup>13</sup> morphologies. The stability of these phases depends on minimization of both molecular packing frustration and interfacial area.<sup>14</sup> Accurate classification of structurally complex morphologies necessarily requires caution, since they may appear identical upon projection in transmission electron microscopy (TEM) or exhibit insufficient long-range order in small-angle scattering to permit unambiguous identification. A recent effort<sup>3</sup> to classify the microstructure of an isoprene-rich poly(styrene-*b*-isoprene) (SI) diblock copolymer has demonstrated that the G morphology, exhibiting *Ia* $\bar{3}d$  symmetry, can be successfully distinguished from the double-diamond (D) morphology, which belongs to the *Pn* $\bar{3}m$  space group, by its small-angle X-ray scattering (SAXS) signature. Such analysis has also resulted in reclassification of two starblock copolymers from the D to the G morphology.<sup>4</sup> A complementary analytical method that has likewise proven valuable in identifying complex block copolymer morphologies in real space is transmission electron microtomography.<sup>6</sup> This technique yields 3-D images of structurally complex and nonperiodic morphologies *in-situ*, without any of the assumptions required in simulations.<sup>15</sup>

In each of these previous studies, the self-organizing molecule has been either an AB diblock or an  $-(AB)_n$  starblock copolymer, composed of two or more chains joined at a single covalent junction. In the microphase-ordered state, each block possesses one “tethered” end, which is constrained to locate in the interfacial region separating adjacent A and B microdomains. Linear multiblock copolymer molecules, on the other hand,

possess at least one midblock that is tethered at both ends. Unlike an endblock, a midblock is biconformational since it is capable of adopting either a bridged or looped conformation. Numerous works have been reported over the past few years in an attempt to discern the impact of midblock conformation (i.e., the “bridging fraction”) and molecular architecture on the microstructural characteristics and bulk properties of ordered ABA triblock copolymers<sup>16–21</sup> (with one midblock/molecule) and (AB)<sub>n</sub> multiblock copolymers<sup>21–25</sup> (with 2n – 2 midblocks/molecule). Previous efforts<sup>26</sup> have shown that triblock copolymer/homopolymer blends appear capable of ordering into a bicontinuous morphology. In the present work, we employ TEM, SAXS, and transmission electron microtomography to analyze a cubic bicontinuous morphology in a neat isoprene-rich SIS triblock copolymer.

The poly(styrene-*b*-isoprene-*b*-styrene) (SIS) triblock copolymer was synthesized in cyclohexane at 60 °C via living anionic polymerization with *sec*-butyllithium. According to <sup>1</sup>H NMR, the copolymer was 33 wt % S, and its  $\bar{M}_n$  and polydispersity index, as measured from GPC, were 92 000 and 1.09, respectively. On the basis of the densities for polystyrene and polyisoprene at 100 °C (1.00 and 0.84 g/cm<sup>3</sup>, respectively<sup>27,28</sup>), we calculate a styrene volume fraction ( $f_s$ ) of 0.32 for this copolymer. For comparison, the  $f_s$  range over which G or D morphologies have been documented<sup>2</sup> for neat isoprene-rich copolymers is 0.31–0.35. Bulk films of the copolymer were prepared from a 4% (wt/vol) toluene solution cast into Teflon molds. After slow solvent removal over the course of 3 weeks, resultant films measuring *ca.* 2 mm thick were dried at 90 °C for 4 h under vacuum. Specimens for TEM and transmission electron tomography were produced by first sectioning the bulk films in a Reichert-Jung Ultracut-S ultramicrotome at –100 °C, and then staining the electron-transparent sections with the vapor of 2% OsO<sub>4</sub>(aq) for 90 min.

Electron micrographs were obtained on a JEOL JEM-200CX transmission electron microscope operated at 120 kV. For microtomography, a series of 49 480 × 480 pixel images was collected at 2.1 nm/pixel at tilt angles ranging from +60° to –60° in 2.5° increments on a computer-controlled Philips 430 electron microscope, operated at 200 kV. It was equipped with a Thomson 1024 × 1024 CCD chip fiber-optically coupled to a single-crystal scintillator. For SAXS analysis, uniformly thick strips cut from the bulk film were subjected to Cu K $\alpha$  radiation from a Rigaku RU-200BH rotating anode instrument with an anode focal spot foreshortened to 0.2 × 0.2 mm<sup>2</sup> and Franks mirror optics. Two-dimensional scattering images, acquired on an image-intensified, CCD-based area detector,<sup>29</sup> were corrected for detector response and integrated azimuthally along an arc  $\pm 15^\circ$  from the horizontal axis to obtain 1-D scattering patterns.

Electron micrographs of the SIS copolymer are presented in Figure 1. The relatively low magnification image shown in Figure 1a reveals the presence of a highly-ordered, single-phase morphology exhibiting surprisingly few defects. At higher magnification (Figure 1b), interpenetrating S (bright) and I (dark) channels are arranged in the “wagon-wheel” pattern commonly associated with the [111] projection of the cubic bicontinuous G and D morphologies.<sup>15</sup> As mentioned earlier, classification of complex cubic morphologies is best achieved by SAXS analysis, providing that sufficient long-range order exists. Figure 2 displays a SAXS

\* To whom correspondence should be addressed.

<sup>†</sup> North Carolina State University.

<sup>‡</sup> Princeton University.

<sup>§</sup> Present address: Department of Chemical Engineering and Materials Science, University of Minnesota, Minneapolis, MN 55455.

<sup>||</sup> Graduate Group in Biophysics, University of California.

<sup>⊥</sup> Department of Biochemistry and Biophysics, University of California.

<sup>○</sup> The Procter and Gamble Company.

<sup>¶</sup> Howard Hughes Medical Institute, University of California.

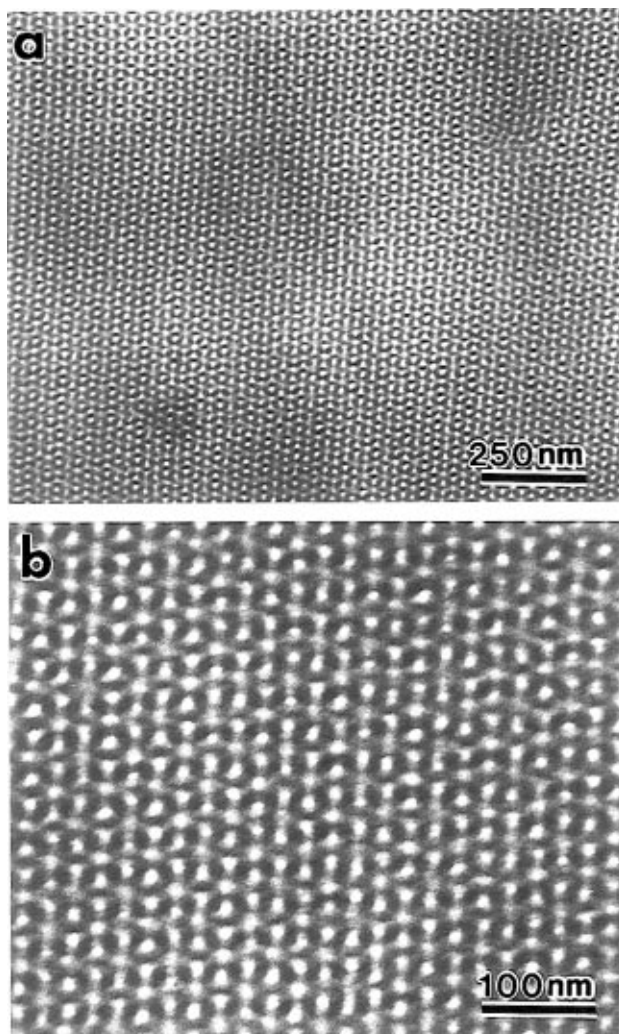


**Figure 1.** Transmission electron micrographs of the SIS triblock copolymer examined in this study. Due to  $\text{OsO}_4$  staining, isoprene-rich regions are electron-opaque and appear dark. At low magnification (a), the morphology appears highly ordered with relatively few defects. In part b, the "wagon-wheel" projection associated with the [111] axis of the G or D morphology is evident.

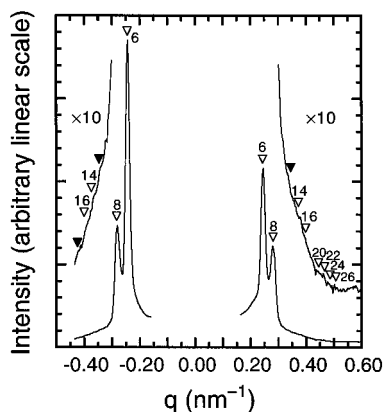


**Figure 2.** Small-angle X-ray scattering profile obtained from the same copolymer displayed in Figure 1. Peak position ratios for the first few orders of the G morphology are identified by ( $\nabla$ ),<sup>3</sup> whereas integral spacing ratios (characteristic of a layered microstructure) are marked with ( $\blacktriangledown$ ). The label on each ( $\nabla$ ) gives the square of the peak position ratio (modulus).

profile obtained from the copolymer at ambient temperature. The open markers identify the square of peak position ratios (moduli) expected for morphologies with

cubic symmetry. This profile exhibits pronounced scattering peaks at spacing ratios of  $\sqrt{3}:\sqrt{4}$ , which is characteristic of the G morphology; the absence of a peak at a ratio of  $\sqrt{2}$  suggests that this is not the D phase.<sup>3,4</sup> The absence of higher order reflections presumably reflects the absence of long-range order within the morphology, despite the existence of relatively large grains (such as the one seen in Figure 1a).

Transmission electron microtomography is a powerful analytical technique that greatly facilitates the real-space structural analysis of complex, 3-D nanoscale morphologies in block copolymer systems, without requiring *a priori* symmetry or surface assumptions.<sup>15</sup> This technique has proven particularly valuable in the study of macromolecular assemblies of biological interest (e.g., chromosomes<sup>30</sup>) and has been extended to the study of both ordered<sup>6</sup> and disordered<sup>13</sup> block copolymers. Details regarding the principles of *r*-weighted (filtered) back-projection reconstruction are provided elsewhere<sup>31,32</sup> and are not reproduced here. Figure 3 shows a series of tilt images from a volume-rendered reconstruction of the morphology produced in the SIS copolymer investigated here. Adjacent images are stereopairs separated by  $20^\circ$  (3-D visualization is enhanced through the use of stereoglasses). This morphology consists of co-interpenetrating channels of the S and I microphases (only the S microphase is shown here for clarity; the I microphase corresponds to the empty volume), and it is reminiscent of the G morphology with  $Ia\bar{3}d$  symmetry reported elsewhere.<sup>3,4,6</sup>

Volumetric analysis of the reconstruction presented in Figure 3 yields  $f_S \approx 0.35$ , in good agreement with the known composition of the copolymer ( $f_S \approx 0.32$ ). An important feature of Figure 3 is the number of channels intersecting at a vertex, since the D and G morphologies are differentiated by the channel coordination of the minority component. The D morphology consists of four channels/vertex, whereas the G possesses only three channels/vertex.<sup>3,14</sup> Close examination of Figure 3 (and of video footage showing other tilt angles) reveals that the channel coordination of this morphology is three, which is consistent with the SAXS data presented in Figure 2 and confirms that this morphology is G. To further demonstrate the complementary nature of the TEM and SAXS data provided here, one final comparison is made. In general, scattering (reciprocal space) data from complex structural elements cannot be used to generate the real-space arrangement of a given microstructure through Fourier reconstruction unless the phase factor for each Fourier component can be specified. However, the reverse is possible: Fourier transformation of real-space images yields the structure factor  $S(q)$ , which is proportional to the scattered intensity.<sup>33</sup>

The structure factor generated from the reconstruction displayed in Figure 3 is presented in Figure 4 and appears qualitatively similar to the SAXS pattern shown in Figure 2. Of particular importance are the maxima located at ca.  $0.24$  and  $0.29 \text{ nm}^{-1}$ . The ratio of these positions ( $\approx 1.2$ ) cannot be quantified to the same level of accuracy ( $(8/6)^{1/2} \approx 1.15$ ) as it is from SAXS, since the data in Figure 4 are at significantly lower resolution than those in Figure 2 (note the resolution marker in the lower left-hand corner of the figure). Thus, the maxima in Figure 2 may not, in fact, correspond to the absolute  $S(q)$  maxima in reciprocal space, since the real-space data used to generate  $S(q)$  are only resolved to  $2.1 \text{ nm/pixel}$ . Due to this present limitation,

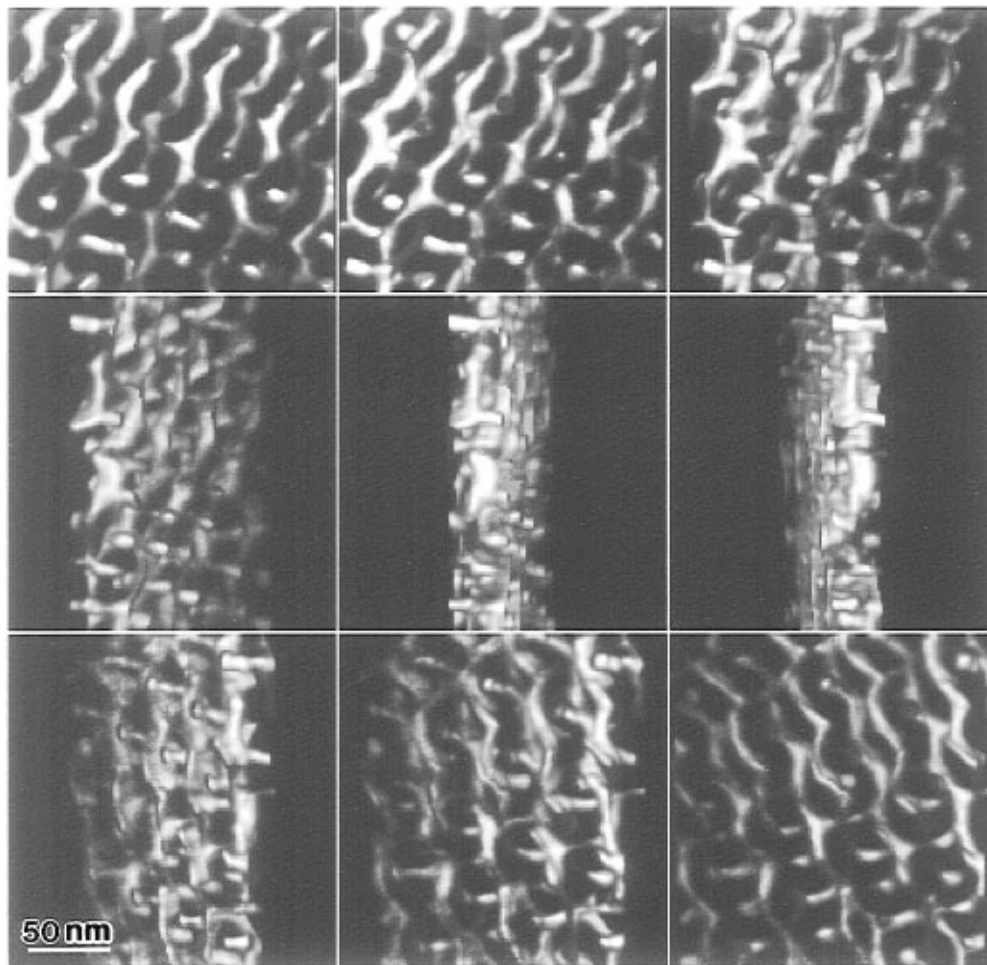


**Figure 3.** Three-dimensional images of the cubic bicontinuous morphology produced in the neat SIS copolymer (33 wt % S) investigated here and obtained through transmission electron microtomography. Solid renderings are provided at 20° tilt angles to facilitate 3-D visualization through the use of stereo glasses. Note that three styrene channels (tubes), each measuring about 7–10 nm in diameter, intersect at every vertex, confirming that this is the G morphology.

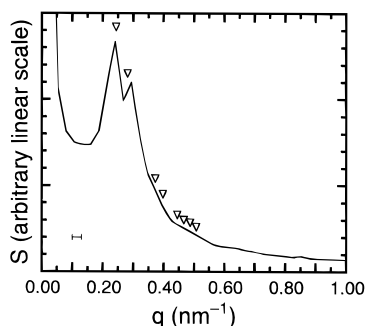


**Figure 4.** Structure factor,  $S(q)$ , of the cubic bicontinuous morphology examined here. It is generated upon Fourier transformation of the 3-D reconstruction displayed in Figure 3. Two maxima are located at  $q$  in close proximity to the primary scattering peaks (at position ratios  $\sqrt{6}$  and  $\sqrt{8}$ ) in the SAXS pattern shown in Figure 2. The resolution of the data presented in this figure is denoted by the bar in the lower left corner, and the ( $\nabla$ ) denote the same G peak position ratios shown in Figure 2.

as well as the possibility of microtomy-induced plastic deformation of the sample (which might conceivably affect the spacings of certain lattice planes), it is not yet possible to use this  $S(q)$  signature to distinguish complex cubic morphologies. Instead, we point out that  $S(q)$  in Figure 4 possesses the characteristics associated with a cubic bicontinuous morphology such as either the G or D. To facilitate further comparison with Figure 2, the markers used to label position ratios pertaining

to cubic bicontinuous morphologies are included in Figure 4.

While recent studies<sup>1–6</sup> have identified the stable composition regime of the G morphology and verified its symmetry in diblock copolymers and copolymer blends residing within this regime, none have, as of yet, demonstrated the existence of this phase in a neat linear multiblock copolymer. On the basis of a self-consistent field analysis, Matsen and Schick<sup>22</sup> predict that linear multiblock copolymers are capable of ordering into stable complex morphologies (such as the G). According to their predictions, the difference in conformational entropy associated with elastomeric endblocks and biconformational midblocks is relatively small, suggesting that the free energy and interfacial modulus<sup>34</sup> of an ABA triblock copolymer exhibiting the G morphology should not differ significantly from those of a comparable AB diblock copolymer exhibiting the same morphology. In this work, we provide evidence that an isoprene-rich SIS triblock copolymer within the same composition range as its diblock analog can order into a structurally complex morphology despite the presence of double-tethered (biconformational) matrix blocks.

**Acknowledgment.** This study has been supported by the Shell Development Co. and the U.S. Department of Energy under contract DE-AC03-76SF00098. R.J.S. thanks the National Center for Electron Microscopy for a Visiting Scientist Award. Work at Princeton was supported by the U.S. Department of Energy under

Contract DE-FG02-87ER60522 and the National Science Foundation (DMR-922-3966). J.C.F., J.W.S., and D.A.A. acknowledge support from the National Institutes of Health (GM31627, D.A.A.; GM25101, J.W.S.), and D.A.A. was supported by the Howard Hughes Medical Institute.

### References and Notes

- (1) Förster, S.; Khandpur, A. K.; Zhao, J.; Bates, F. S.; Hamley, I. W.; Ryan, A. J.; Bras, W. *Macromolecules* **1994**, *27*, 6922.
- (2) Khandpur, A. K.; Förster, S.; Bates, F. S.; Hamley, I. W.; Ryan, A. J.; Bras, W.; Almdal, K.; Mortensen, K. *Macromolecules* **1995**, *28*, 8796.
- (3) Hajduk, D. A.; Harper, P. E.; Gruner, S. M.; Honeker, C. C.; Kim, G.; Thomas, E. L.; Fetters, L. J. *Macromolecules* **1994**, *27*, 4063.
- (4) Hajduk, D. A.; Harper, P. E.; Gruner, S. M.; Honeker, C. C.; Thomas, E. L.; Fetters, L. J. *Macromolecules* **1995**, *28*, 2570.
- (5) Zhao, J.; Majumdar, B.; Schulz, M. F.; Bates, F. S.; Almdal, K.; Mortensen, K.; Hajduk, D. A.; Gruner, S. M. *Macromolecules* **1996**, *29*, 1204.
- (6) Spontak, R. J.; Fung, J. C.; Braunfeld, M. B.; Sedat, J. W.; Agard, D. A.; Kane, L.; Smith, S. D.; Satkowski, M. M.; Ashraf, A.; Hajduk, D. A.; Gruner, S. M. *Macromolecules* **1996**, *29*, 4494.
- (7) Hamley, I. W.; Koppi, K. A.; Rosedale, J. H.; Bates, F. S.; Almdal, K.; Mortensen, K. *Macromolecules* **1993**, *26*, 5959.
- (8) Hamley, I. W.; Gehlsen, M. D.; Khandpur, A. K.; Koppi, K. A.; Rosedale, J. H.; Schulz, M. F.; Bates, F. S.; Almdal, K.; Mortensen, K. *J. Phys. II (Fr.)* **1994**, *4*, 2161.
- (9) Hajduk, D. A.; Takenouchi, H.; Hillmyer, M. A.; Bates, F. S.; Vigild, M. E.; Almdal, K. *Macromolecules* **1997**, *30*, 3788–3795.
- (10) Thomas, E. L.; Anderson, D. M.; Henkee, C. S.; Hoffman, D. *Nature* **1988**, *334*, 598.
- (11) Spontak, R. J.; Smith, S. D.; Ashraf, A. *Macromolecules* **1993**, *26*, 956.
- (12) Disko, M. M.; Liang, K. S.; Behal, S. K.; Roe, R.-J.; Jeon, K. *Macromolecules* **1993**, *26*, 2983.
- (13) Laurer, J. H.; Fung, J. C.; Sedat, J. W.; Agard, D. A.; Smith, S. D.; Samseth, J.; Mortensen, K.; Spontak, R. *J. Langmuir* **1997**, *13*, 2177.
- (14) Matsen, M. W.; Bates, F. S. *Macromolecules* **1996**, *29*, 7641.
- (15) Anderson, D. M.; Bellare, J.; Hoffman, J. T.; Hoffman, D.; Gunther, J.; Thomas, E. L. *J. Colloid Interface Sci.* **1992**, *148*, 398.
- (16) Zhulina, E. B.; Halperin, A. *Macromolecules* **1992**, *25*, 5730.
- (17) Matsen, M. W.; Schick, M. *Macromolecules* **1994**, *27*, 187.
- (18) Lee, S. H.; Koberstein, J. T.; Quan, X.; Gancarz, I.; Wignall, G. D.; Wilson, F. C. *Macromolecules* **1994**, *27*, 3199.
- (19) Watanabe, H. *Macromolecules* **1995**, *28*, 5006.
- (20) Jones, R. L.; Kane, L.; Spontak, R. J. *Chem. Eng. Sci.* **1996**, *51*, 1365.
- (21) For a recent compilation of block copolymer morphologies and architectures, see: Schulz, M. F.; Bates, F. S. In *Physical Properties of Polymers Handbook*; Mark, J. E., Ed.; American Institute of Physics Press: New York, 1996; Chapter 32.
- (22) Matsen, M. W.; Schick, M. *Macromolecules* **1994**, *27*, 7157.
- (23) Smith, S. D.; Spontak, R. J.; Satkowski, M. M.; Ashraf, A.; Lin, J. S. *Phys. Rev. B* **1993**, *47*, 14555. Smith, S. D.; Spontak, R. J.; Satkowski, M. M.; Ashraf, A.; Heape, A. K.; Lin, J. S. *Polymer* **1994**, *36*, 4527.
- (24) Matsushita, Y.; Mogi, Y.; Mukai, H.; Watanabe, J.; Noda, I. *Polymer* **1994**, *35*, 246.
- (25) Matsen, M. W. *J. Chem. Phys.* **1995**, *102*, 3884.
- (26) Xie, R.; Yang, B. X.; Jiang, B. Z. *Macromolecules* **1993**, *26*, 7097.
- (27) Boothroyd, A.; Rennie, A.; Wignall, G. D. *J. Chem. Phys.* **1993**, *91*, 9135.
- (28) Fetters, L. J.; Lohse, D. J.; Richter, D.; Witten, T. A.; Zirkel, A. *Macromolecules* **1994**, *27*, 4639.
- (29) Tate, M. W.; Gruner, S. M.; Eikenberry, E. F. *Rev. Sci. Instrum.* **1997**, *68*, 47.
- (30) Horowitz, R. A.; Agard, D. A.; Sedat, J. W.; Woodcock, C. L. *J. Cell. Biol.* **1994**, *125*, 1.
- (31) Frank, J., Ed. *Electron Tomography: Three-Dimensional Imaging with the Transmission Electron Microscope*; Plenum: New York, 1992.
- (32) Fung, J. C.; Liu, W.; deRuijter, W. J.; Chen, H.; Abbey, C. K.; Sedat, J. W.; Agard, D. A. *J. Struct. Biol.* **1996**, *116*, 181.
- (33) Jinnai, H.; Nishikawa, Y.; Koga, T.; Hashimoto, T.; *Macromolecules* **1995**, *28*, 4782.
- (34) Matsen, M. W.; Schick, M. *Macromolecules* **1993**, *26*, 3878; **1994**, *27*, 2316.

MA970449L